

A general two-stream algorithm for retrieving spectral surface albedo

Zhanqing Li, Howard W. Barker, and Louis Moreau

Abstract. Spectral surface albedo (SSA) has numerous applications in climate and environmental studies. Given that ground-based observations of SSA are very limited, space-borne remote sensing has been the primary means of acquiring SSA on large or global scales. To date, many satellite sensors measure reflectances in different spectral regions from which values of SSA are inferred. The inversion algorithms range from simple linear relationships to complex, full-fledged radiative transfer models. Often, algorithms were designed for application to a particular sensor or spectral band. In this study, we propose a more versatile parameterized algorithm that can be used for estimating SSA from satellite-measured spectral albedos at the top of the atmosphere (TOA). The algorithm was developed based on a three-layer atmospheric model. Monochromatic and band transmittances due to various absorbing species are parameterized. The reflectance and transmittance for direct and diffuse radiation in the second layer are determined by the generalized two-stream solutions. Except for the parameterization coefficients that vary with the bandpass and spectral response function of the satellite sensor, the framework of the inversion model is applicable to any sensor or spectral region. The model is tested by applying it to the results of detailed radiative transfer simulations for a wide range of conditions for various satellite sensors and spectral bands. The complexity and accuracy of the proposed model are intermediate relative to those of models currently in use.

Résumé. L'albédo spectral de surface (SSA) a plusieurs applications dans les études climatiques ou environnementales. Étant donné que les observations de SSA au sol sont très limitées, la télédétection satellitaire constitue le moyen privilégié d'acquisition de SSA à grande échelle ou à l'échelle du globe. Aujourd'hui, plusieurs capteurs satellitaires mesurent les réflectances dans différentes bandes spectrales à partir desquelles la valeur de SSA est déduite. Les algorithmes d'inversion varient des simples relations linéaires aux modèles plus complexes de transfert radiatif. Souvent, les algorithmes ont été développés pour application à un capteur particulier ou une bande spectrale spécifique. Dans cette étude, nous proposons un algorithme de paramétrage plus versatile qui peut être utilisé pour l'estimation de SSA à partir de mesures d'albédo spectral acquises par satellite au sommet de l'atmosphère (TOA). L'algorithme a été développé à partir d'un modèle atmosphérique à trois couches. Les transmittances monochromatiques et intégrées sur la bande dues aux différentes composantes absorbantes de l'atmosphère sont paramétrées. La réflectance et la transmittance du rayonnement direct et diffus dans la seconde couche sont déterminées au moyen de solutions généralisées à deux flux. À l'exception des coefficients de paramétrisation qui varient en fonction de la largeur de la bande et de la fonction de réponse spectrale du capteur satellitaire, le cadre du modèle d'inversion est applicable à n'importe quel capteur ou région spectrale. Le modèle est testé en l'appliquant aux résultats de simulations détaillées de transfert radiatif pour une grande variété de conditions et pour divers capteurs satellitaires et diverses bandes spectrales. La complexité et la précision du modèle sont intermédiaires par rapport à ce que l'on utilise à l'heure actuelle.

[Traduit par la Rédaction]

Introduction

The needs for spectral surface albedo (SSA) are multifold. First, the spectral variation of surface albedo is a unique signature of the target. Such a signature has been widely used in a variety of remote sensing applications. A chief example is the use of vegetation indices (VIs), which are often derived from measurements in two spectral bands, namely the visible (VIS) and near infrared (NIR) (Huete et al., 2002). The utilities of VIs in remote sensing are numerous, ranging from the retrieval of bio-geo-physical parameters (e.g., photosynthetically active radiation or PAR) (Li et al., 1997a) to the classification of land cover types (Cihlar et al., 1997a; 1997b). SSA is a fundamental input variable for inferring atmospheric parameters (cloud, aerosol, water vapour, etc.) from multispectral space-borne observations (Kaufman et al., 2002; King et al., 2003; Remer et al., 2005). It is because of inadequate knowledge of SSA that

some remote sensing applications, such as aerosol optical thickness, have been limited to relatively uniform ocean surfaces (Nakajima and Higurashi, 1998; Mishchenko et al., 2003; Jeong and Li, 2005). Closure tests of radiative transfer calculations cannot be achieved unless SSA is known, especially under cloudy conditions due to multiple internal

Received 31 January 2005. Accepted 2 August 2005.

Z. Li.¹ Department of Atmospheric and Oceanic Science, University of Maryland, College Park, MD 20742, USA.

H.W. Barker. Meteorological Service of Canada, Downsview, ON, M3H 5T4, Canada.

L. Moreau. Intermap Information Corporation, Nepean, ON K2E 1A2, Canada.

¹Corresponding author (e-mail: zli@atmos.umd.edu).

reflections between surface and atmosphere (Barker and Davies, 1989; Li et al., 2002).

As general circulation models (GCMs) advance, there is an increasing demand for high-resolution SSA data from satellites (Dickerson et al., 1990). Not long ago, two-band GCMs were typical, but now GCMs with four or more bands are more popular (Barker et al., 2003). Modelling Earth's climate and understanding the feedbacks between climate and land surface require a good knowledge of SSA on the global scale (Dickerson, 1983). A substantial amount of discrepancy in the simulation of Earth's energy budget originates from large differences in surface albedo datasets used by various GCMs (Li et al., 1997b). It is highly desirable to derive an accurate, global, spectral, and broadband albedo climatology to facilitate climate change studies (Sellers, 1985).

Satellite remote sensing remains a primary tool to meet the aforementioned requirements. Note that there are several steps to convert satellite-measured radiances to surface albedos, although an alternative approach was proposed recently to circumvent the steps by directly linking planetary reflectance with surface albedo following a hybrid modelling and statistical method (Liang, 2003). They include corrections of the spectral response function of the sensor (Trishchenko et al., 2002), the atmospheric effects (Vermote et al., 1997), conversion of reflectance as measured from a particular direction to an albedo defined over the entire hemisphere, or the commonly known bidirectional reflectance distribution function (Luo et al., 2005). If a broadband albedo is derived from narrow-band measurements, spectral conversion is required (Li and Trishchenko, 1999; Liang et al., 2005). Uncertainties are incurred in any of these steps. This study deals with one of the steps, namely, converting a planetary albedo into a surface albedo following atmospheric correction, assuming that the angular correction has been applied to convert the satellite-measured reflectance to a planetary albedo. Although most BRDF models are for broadband radiances, a limited number of BRDF models have also been proposed (e.g., Chang et al. (2000) for the visible region and Ciren and Li (2001) for the ultraviolet region).

At present, there exist some global broadband surface albedo datasets derived from various satellite sensors and systems such as the Earth Radiation Budget Experiment (ERBE) (Li and Garand, 1994), the International Satellite Cloud Climatology Project (ISCCP) (Pinker and Laszlo, 1992), and the moderate-resolution imaging spectroradiometer (MODIS) (Schaaf et al., 2002), in addition to many regional albedo estimates (e.g., Barker and Davies, 1989). Most notable is MODIS, which has 36 channels, 23 of which are located at solar wavelengths up to 4.0 μm . SSA is one of the MODIS products following atmospheric correction (Vermote et al., 1997) and bidirectional correction (Lucht et al., 2000; Li et al., 2001).

The purpose of this study is to propose a satellite-based algorithm for retrieving SSA. The algorithm is intended for general application, instead of being tailored for a particular sensor. For a given satellite radiometer, the spectral filter function is required to derive specific coefficients in the

parameterization schemes proposed in the paper. In terms of complexity, the proposed model is intermediate between the simple highly parameterized models (Chen and Ohring, 1984; Li and Garand, 1994) and more complicated radiative transfer models (Vermote et al., 1997), or a feed-forward neural network (Liang et al., 1999). The model developed here is more versatile and accurate relative to the simple parameterized models and at the same time involves less computation and fewer input parameters relative to the complicated models. Given that the parameters characterizing the state of the atmosphere contain many uncertainties, even in the era of Earth-observing systems (EOS), the model presented is of certain special utility.

Model

This model is based on a three-layer atmosphere–surface system as depicted in **Figure 1**. The top layer consists of ozone molecules that attenuate solar radiation due to absorption at some specific wavelengths. The radiative properties of this layer can thus be characterized by transmittance functions T_1 and T_1^* for direct and diffuse solar irradiance, respectively. For monochromatic radiation, transmittance due to ozone absorption is determined by Beer's law. The middle layer contains radiatively active constituents including air molecules, water vapour, CO_2 and other gases, and aerosols. These agents have strong interactions via scattering and absorption. The bulk radiative properties of this layer include reflectance and transmittance for direct (R_2 and T_2) and diffuse (R_2^* and T_2^*) sunlight. The third layer is the surface whose albedo (R_g) is to be derived.

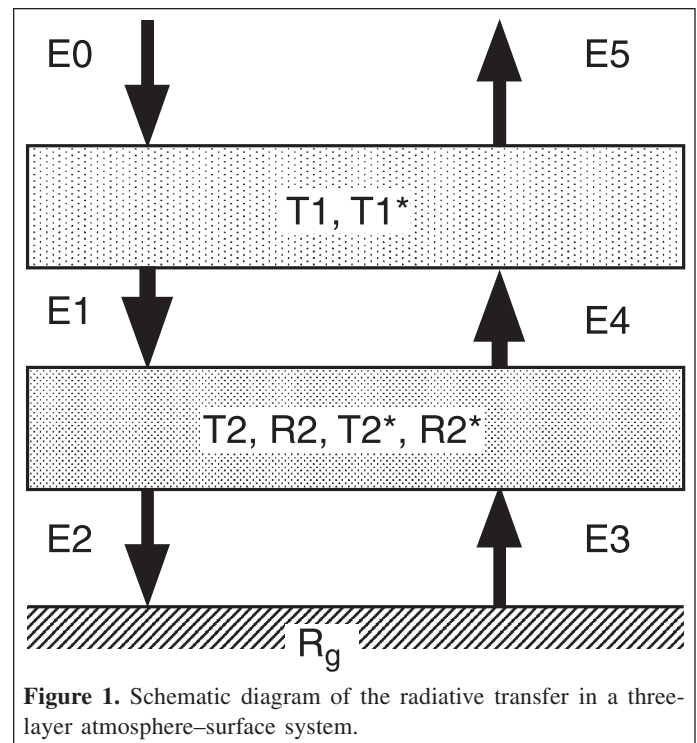


Figure 1. Schematic diagram of the radiative transfer in a three-layer atmosphere–surface system.

For such a system, the following six equations govern the transfer of fluxes between three levels:

$$\left. \begin{aligned} E_0 &= 1 \\ E_1 &= T_1 E_0 \\ E_2 &= T_2 E_1 + R_2^* E_3 \\ E_3 &= R_s E_2 \\ E_4 &= T_2^* E_3 + R_2 E_1 \\ E_5 &= T_1^* E_4 \end{aligned} \right\} \quad (1)$$

from which surface albedo is solved as an analytic function of the planetary albedo ($R_p = E_5$) and other atmospheric radiative quantities:

$$R_p = T_1 T_1^* \left(R_2 + \frac{R_s T_2 T_2^*}{1 - R_s R_2^*} \right) \quad (2)$$

$$R_s = \frac{R_p - R_2 T_1 T_1^*}{R_2^* (R_p - R_2 T_1 T_1^*) + T_2 T_2^* T_1 T_1^*} \quad (3)$$

Reflectance and transmittance of the middle layer can be solved by a generalized two-stream approximation for any set of single-scattering properties, namely optical thickness, single-scattering albedo, and asymmetry factor (Meador and Weaver, 1980). Since the layer contains several atmospheric species, its total optical thickness (τ) is the sum of individual thicknesses:

$$\tau = \tau_a + \tau_R + \tau_{H_2O} + \tau_{CO_2} + \tau_{abs} \quad (4)$$

where the variables on the right-hand side represent optical thicknesses of aerosols (τ_a), atmospheric molecules (Rayleigh scattering) (τ_R), water vapour (τ_{H_2O}), carbon dioxide (τ_{CO_2}), and other absorbing materials (τ_{abs}). Their values are discussed in the following section. Effective values for single-scattering albedo (ω) and asymmetry factor (g) for the layer are given by the following (Leighton, 1980):

$$\omega = \frac{\omega_a \tau_a + \tau_R}{\tau} \quad (5)$$

$$g = \frac{g_a \omega_a \tau_a}{\omega \tau} \quad (6)$$

where ω_a and g_a are single-scattering albedo and asymmetry factors, respectively, for aerosols. With these single-scattering quantities, the generalized two-stream solutions for the second layer are as follows:

$$R_2(\mu_0) = \frac{\omega r_+ \exp(k\tau) - r_- \exp(-k\tau) - r_0 \exp(-\tau/\mu_0)}{a \exp(k\tau) - \beta \exp(-k\tau)}, \quad (7)$$

$$T_2(\mu_0) = \exp(-\tau/\mu_0) \times \left[1 - \frac{\omega t_+ \exp(k\tau) - t_- \exp(-k\tau) - t_0 \exp(-\tau/\mu_0)}{\exp(k\tau) - \beta \exp(-k\tau)} \right], \quad (8)$$

$$R_2^* = \frac{\gamma_2}{k + \gamma_1} \frac{1 - \exp(-2k\tau)}{1 - \beta \exp(-2k\tau)}, \quad (9)$$

$$T_2^* = \frac{2k}{k + \gamma_1} \frac{\exp(-k\tau)}{1 - \beta \exp(-2k\tau)}, \quad (10)$$

where $r_{\pm} = (1 \mp k\mu_0)(\gamma_1\gamma_3 - \gamma_2\gamma_4 \pm k\gamma_3)$, $r_0 = 2k[\gamma_3 - (\gamma_1\gamma_3 - \gamma_2\gamma_4)\mu_0]$, $t_{\pm} = (1 \pm k\mu_0)(\gamma_1\gamma_4 - \gamma_2\gamma_3 \pm k\gamma_4)$, $t_0 = 2k[\gamma_4 - (\gamma_1\gamma_4 - \gamma_2\gamma_3)\mu_0]$, $a = [1 - (k\mu_0)^2](k + \gamma_1)T$, $k = (\gamma_1^2 - \gamma_2^2)^{0.5}$, $\beta = -(k - \gamma_1)/(k + \gamma_1)$, $\gamma_1, \dots, \gamma_4$ depend on the choice of a two-stream method; and μ_0 is the cosine of the solar zenith angle. For the delta-Eddington approximation (Joseph et al., 1976),

$$\left. \begin{aligned} k &= \frac{1}{2} \sqrt{3(1 - \omega'_0)(1 - \omega'g')} \\ \gamma_1 &= \frac{7 - \omega'(4 + 3g')}{4} \\ \gamma_2 &= \frac{1 - \omega'(4 - 3g')}{4} \\ \gamma_3 &= \frac{2 - 3\mu_0 g'}{4} \\ \gamma_4 &= 1 - \gamma_3 \end{aligned} \right\} \quad (11)$$

in which

$$\left. \begin{aligned} \tau' &= (1 - \omega g^2)\tau \\ \omega' &= \frac{\omega(1 - g^2)}{1 - \omega g^2} \\ g' &= \frac{g}{1 + g} \end{aligned} \right\} \quad (12)$$

The values of transmittance due to absorption are available from precalculated look-up tables using such standard codes as LOWTRAN7 or MODTRAN4. In this study, we used LOWTRAN7 because it has been implemented in our double-adding code, which is used for validation tests under a wide range of conditions. The spectral interval is 25 cm^{-1} for LOWTRAN7. The tables span from 2000 cm^{-1} ($5 \mu\text{m}$) to $50\,000 \text{ cm}^{-1}$ ($0.2 \mu\text{m}$). The look-up tables were generated for varying amounts of gases embedded in the standard atmosphere. Transmittance for any amount of an absorbing gas is determined by a spline interpolation method.

Since transmittance over narrow spectral intervals as used in LOWTRAN7 can be approximated by Beer's law, the optical

thickness for absorbing species can be easily obtained. For example, the optical thickness for ozone is

$$\tau_{O_3} = -\mu_0 \ln[T(O_3/\mu_0)] \tag{13}$$

where T denotes the mean ozone transmittance from look-up tables, and O_3 is the vertical depth of the ozone. Likewise, we can obtain the optical thickness for other gases such as water vapour and CO_2 . The aerosol optical properties are treated as input variables and have been retrieved with a reasonable accuracy over some relatively dark surfaces (e.g., Remer et al., 2005).

Having spectral values of the optical properties for all the components, one can solve for surface albedo averaged over the bandpass of a sensor by spectrally integrating Equation (2) with a weighting factor of the product of the incoming solar irradiance $S(\lambda)$ and sensor filter function $f(\lambda)$. This is achieved by solving

$$\frac{\sum_{j=1}^J S(\lambda_j) f(\lambda_j) T_1(\lambda_j) T_1^* \{R_2(\lambda_j) + [T_2(\lambda_j) T_2^* R_s] / [1 - R_2^* R_s]\}}{\sum_{j=1}^J S(\lambda_j) f(\lambda_j)} - R_p = 0 \tag{14}$$

where λ is the wavelength. This equation can be solved numerically rather quickly by Newton's method. Using planetary albedo as an initial guess for surface albedo, it takes typically only two iterations of computation for R_s to converge to an accuracy of 10^{-5} .

Note that the same approach may not be applied to Equation (3) to compute surface albedo directly due to the strong spectral dependence of planetary albedo, especially at shorter wavelengths because of Rayleigh scattering and scattering by fine aerosol particles. An unphysical value (i.e., larger than unity) would be obtained for a band containing strong absorption lines. Over a narrow band without strong absorption, the two approaches end up with similar results. If weighted spectral integration is conducted for each individual term in Equation (3), however, the resulting surface albedo is very close to that from Equation (14) for any band.

For the narrow bandwidths of many remote sensing instruments, spectrally integrated effective radiative values may be used. They are obtained by averaging over the sensor band (λ_1, λ_2) weighted by $S(\lambda)$ and $f(\lambda)$:

$$\varphi = \frac{\int_{\lambda_1}^{\lambda_2} S(\lambda) f(\lambda) \tilde{\varphi}(\lambda) d\lambda}{\int_{\lambda_1}^{\lambda_2} S(\lambda) f(\lambda) d\lambda}, \tag{15}$$

where $\tilde{\varphi}(\lambda)$ is the spectral-dependent radiative variable under study.

Determination of band-mean reflectance and transmittance

Effective optical properties for direct solar radiation

Gases absorption

The effective direct transmittance due to ozone absorption over a sensor's bandpass is approximated by

$$T_1 = \frac{\int_{\lambda_2}^{\lambda_1} S(\lambda) f(\lambda) \exp(-\tau_{\lambda_{O_3}} r_{O_3} / \mu_0) d\lambda}{\int_{\lambda_2}^{\lambda_1} S(\lambda) f(\lambda) d\lambda} \tag{16}$$

The direct effective monochromatic optical thickness is then derived from T_1 as

$$\tau_{O_3} = -\frac{1}{\mu_0} \ln T_1 \tag{17}$$

Likewise, we can obtain the effective transmittance and optical thickness for water vapour, CO_2 , and other absorbing gases, as well as aerosols. Since the spectral function of the direct solar energy transmitting into the second layer is modified by the overlaying ozone, the weighting function in the spectral integration of the monochromatic transmittance includes the transmittance of the ozone layer, in addition to the top of the atmosphere (TOA) incoming solar spectrum. The direct transmittance due to water vapour absorption, for example, is given by

$$T_{H_2O} = \frac{\int_{\lambda_2}^{\lambda_1} S(\lambda) f(\lambda) \exp(-\tau_{\lambda_{O_3}} r_{O_3} / \mu_0) \exp(-\tau_{\lambda_{H_2O}} r_{H_2O} / \mu_0) d\lambda}{\int_{\lambda_2}^{\lambda_1} S(\lambda) f(\lambda) \exp(-\tau_{\lambda_{O_3}} r_{O_3} / \mu_0) d\lambda} \tag{18}$$

where $\tau_{\lambda_{H_2O}}$ is the monochromatic optical thickness of water vapour absorption read from the look-up table; and r_{H_2O} is the specified amount of water vapour divided by the reference amount of water vapour, which was set at 2.34 g-cm^{-2} in this investigation.

Rayleigh optical depth

Spectral Rayleigh optical depths for the standard atmosphere are approximated as (Hansen et al., 1983)

$$\tau_{R,o}(\lambda) = 0.008569\lambda^{-4}(1 + 0.0113\lambda^{-2} + 0.00013\lambda^{-4}) \tag{19}$$

Values of τ_R for any atmosphere are equal to $(P/P_0)\tau_{R,0}$, where P is the actual surface air pressure, and $P_0 = 1013.25$ mbar (1 bar = 100 kPa). The corresponding monochromatic reflectance for a direct beam is given by

$$R_R[\mu_0, \tau_R(\lambda)] = \frac{3\tau_R(\lambda) + (2 - 3\mu_0)\{1 - \exp[-\tau_R(\lambda)/\mu_0]\}}{4 + 3\tau_R(\lambda)} \quad (20)$$

The effective reflectance over the sensor bandpass is determined by

$$R_R[\mu_0] = \frac{\int_{\lambda_1}^{\lambda_2} S(\lambda)f(\lambda)R[\mu_0, \tau_R(\lambda)]d\lambda}{\int_{\lambda_1}^{\lambda_2} S(\lambda)f(\lambda)d\lambda} \quad (21)$$

Effective optical thickness for diffuse solar radiation

The diffuse flux incident into the middle level is the flux reflected by the surface. The flux incoming on the surface is the sum of the direct flux transmitted through the middle layer and the flux diffused downward by aerosol particles and atmospheric molecules. The direct spectral transmittance is

$$T_{\lambda_2} = \exp\left(-\frac{\tau_{\lambda_2}}{\mu_0}\right) \quad (22)$$

where τ_{λ_2} is the sum of the monochromatic optical thickness of the components in the lower layer (aerosol, water vapour, CO_2 , and air molecules). The fraction of the flux diffused downward is approximated by a single scattering process:

$$F_{\lambda_2} = 0.5[1 - \exp(-\tau_{\lambda_R}/\mu_0)] + [1 - \beta(\lambda, \mu_0)] \times \omega_\lambda[1 - \exp(-\tau_{\lambda_a}/\mu_0)] \quad (23)$$

where τ_{λ_R} is the monochromatic optical thickness of the Rayleigh scatterers, ω_λ is the single scattering albedo of the aerosol at the wavelength λ , τ_{λ_a} is the monochromatic optical thickness of the aerosol, and β is the fraction of radiation backscattered by the aerosol. Assuming the Henyey–Greenstein phase function, β is obtained by integrating the function over the upper hemispheric domain:

$$\beta(\lambda, \mu) = \frac{(1 - g_\lambda^2)}{4g_\lambda(g_\lambda^2 + 2g_\lambda + 1)^{0.5}} - \frac{1}{2} + (g_\lambda^2 + 2g_\lambda \sin \theta_0 + 1)^{-0.5} + (g_\lambda^2 - 2g_\lambda \sin \theta_0 + 1)^{-0.5} \quad (24)$$

where g_λ is the asymmetry factor of the aerosol at the wavelength λ , and θ_0 is the solar zenith angle.

Over a narrow spectral interval, it is assumed that the surface does not alter the spectral dependence of the upwelling flux. As

such, the weighting factors used to determine the diffuse effective transmittance and optical thickness of the radiative constituents in the middle layer should include the sum of T_{λ_2} and F_{λ_2} , in addition to the transmittance due to ozone absorption.

Diffuse equivalent optical thickness for ozone

The upwelling diffuse irradiance onto the ozone layer has two origins, namely backscatter by the aerosol and the Rayleigh scatterers and reflection from the surface. Both of these affect the spectral distribution of the diffuse radiation incoming in the ozone layer.

For the diffuse flux passing through the middle layer, the transmittance $T_{\lambda_2}^*$ is

$$T_{\lambda_2}^* = \exp(-D\tau_{\lambda_2}) \quad (25)$$

where $D = 1.66$ is the diffusivity factor. The backscattered fraction of the downward radiation incoming in the middle layer is

$$B_{\lambda_2} = 0.5[1 - \exp(-\tau_{\lambda_R}/\mu_0)] + \beta(\lambda, \mu_0)\omega_\lambda[1 - \exp(-\tau_{\lambda_a}/\mu_0)] \quad (26)$$

so the total weighting factor to be used in Equation (12) is

$$\exp(-\tau_{\lambda_{O_3}} r_{O_3}/\mu_0)[(T_{\lambda_2} + F_{\lambda_2})T_{\lambda_2}^* + B_{\lambda_2}] \quad (27)$$

For upwelling radiation reflected by the surface, the effective τ in Equations (4)–(6) is approximated by

$$\tau_{H_2O}^\uparrow \equiv -\frac{1}{D} \log \left[\frac{T(w_{H_2O}/\mu_0 + Dw_{H_2O})}{T(w_{H_2O}/\mu_0)} \right] \quad (28)$$

Assuming Lambertian surface reflectance, D varies between 1.50 (thick limit) and 2.00 (thin limit); $D = 1.66$ is used in practice.

Evaluation

The analytic model described herein is evaluated by applying it to TOA reflectances computed by an adding–doubling radiative transfer model (Li and Garand, 1994). To this end, we conducted a large number of simulations with different atmospheric and surface conditions. The latter is specified by the spectral functions of surface albedo for some typical land cover types such as green vegetation, barren land, desert, and snow (Li et al., 2002). These types are considered as input to the radiative transfer model from which the TOA albedos were computed. The computed albedos were then substituted into the parameterized model to estimate surface albedos.

Figure 2 shows the relationship between TOA and surface albedo. The model was run for 292 different combinations of

solar zenith angles ranging from 0° to 70°, surface albedos from 0.05 to 0.98, aerosol optical thicknesses from 0.00 to 0.68, and ozone amount from 0.16 to 0.50 cm. The two variables are shown to have an approximately linear relationship. A great deal of variation in the TOA albedo cannot be explained by the changes in surface albedo, however. Therefore, use of a simple linear regression may result in a large uncertainty in the estimates of surface albedo from TOA albedo, or vice versa. The values of the regression coefficient R^2 , mean bias, and random errors are 0.953, 0.021, and 0.111, respectively, should one apply a simple linear regression to estimate the surface albedos.

Figure 3 shows the surface albedos calculated by the model presented here compared with the true surface albedos used in the radiative transfer model simulations. The improvement over **Figure 2** is significant. The model is able to take into account most of the atmospheric and solar zenith angle effects. Some discrepancies remain (mainly for large solar zenith angles and aerosol loadings), but overall the performance is sound. The values of R^2 , bias, and random errors are 0.997, 0.026, and 0.021, respectively, which are improvements over those from the simple linear regression model.

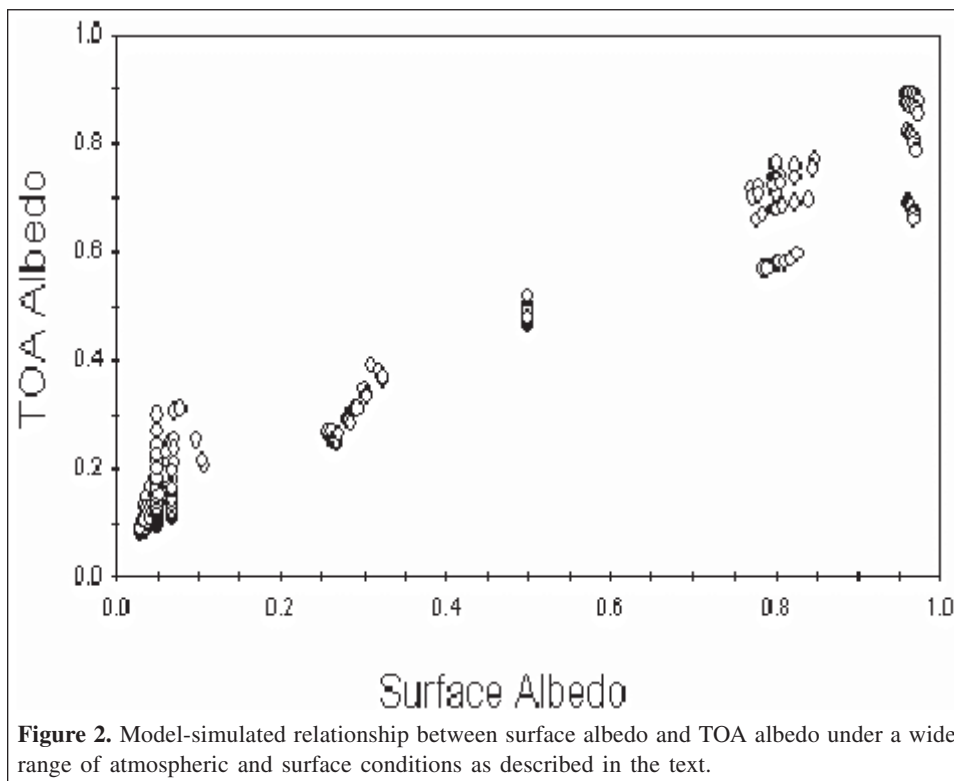
To test the performance of the model in different spectral regions, we applied it to the ultraviolet (UV, 320–400 nm), visible (400–700 nm), and near infrared (NIR, 700–1100 nm) spectral bands and the entire solar spectrum (0–26 000 nm). A comparison of the input and estimated spectral albedos is presented in **Figure 4**. Overall, the performance is good. The best and worst performance correspond to no or weak absorption bands (UV and visible) and strong absorption bands (NIR). This is because the parameterizations suffer from some

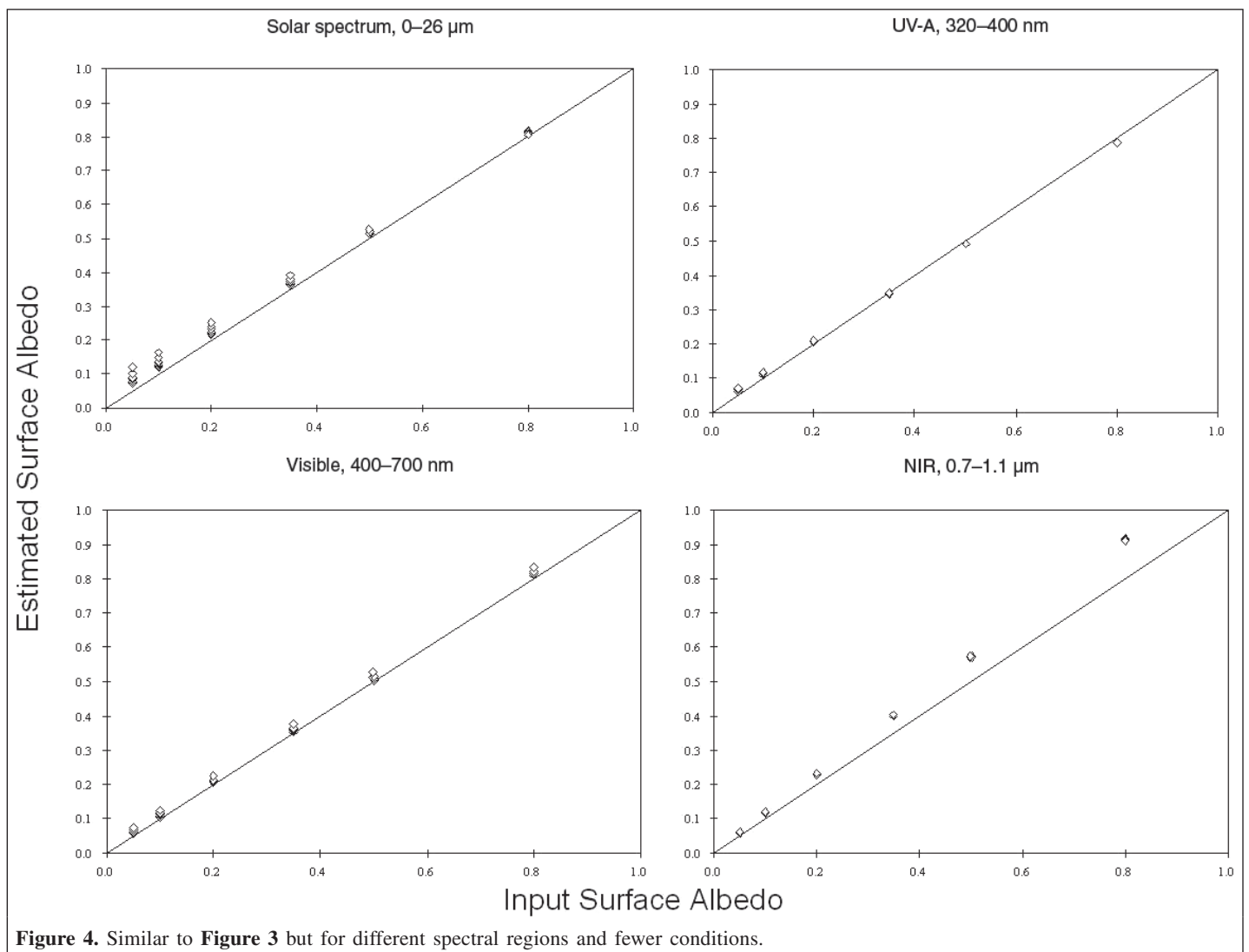
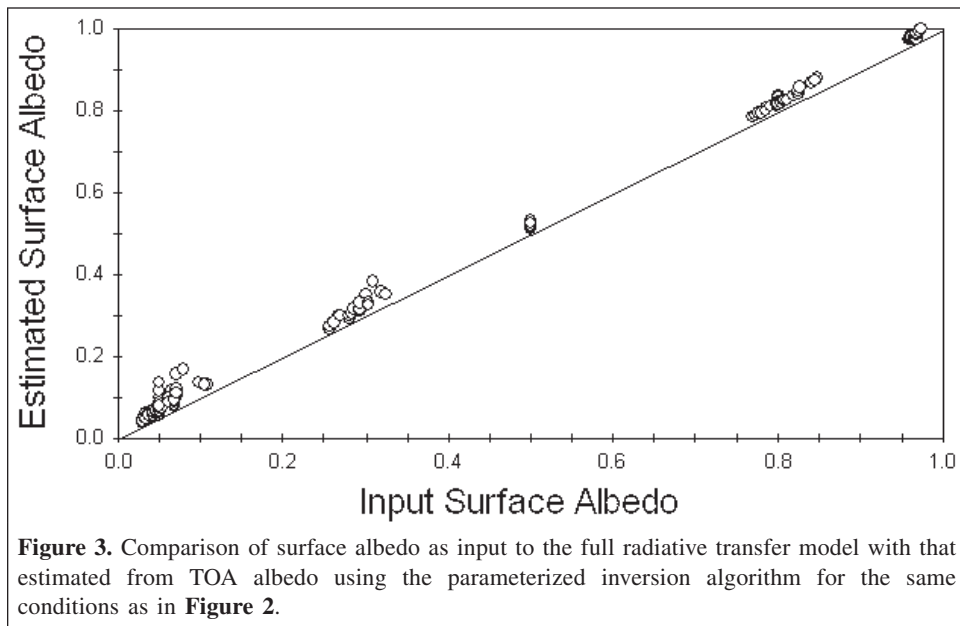
deficiencies due to the strong spectral variation of atmospheric transmittances over fairly wide bands. Fortunately, the majority of sensors used at present have much narrower bandwidths, so in practice estimation errors are expected to be less than those shown here. This is confirmed in **Figure 5**, which shows similar comparisons but for narrower spectral regions, including the advanced very high resolution radiometer (AVHRR) visible channel and 0.7–0.8, 0.8–0.9, and 0.9–1.1 μm . Other simulations (not shown) indicate that the performance of the model depends on water vapour amount and aerosol loading.

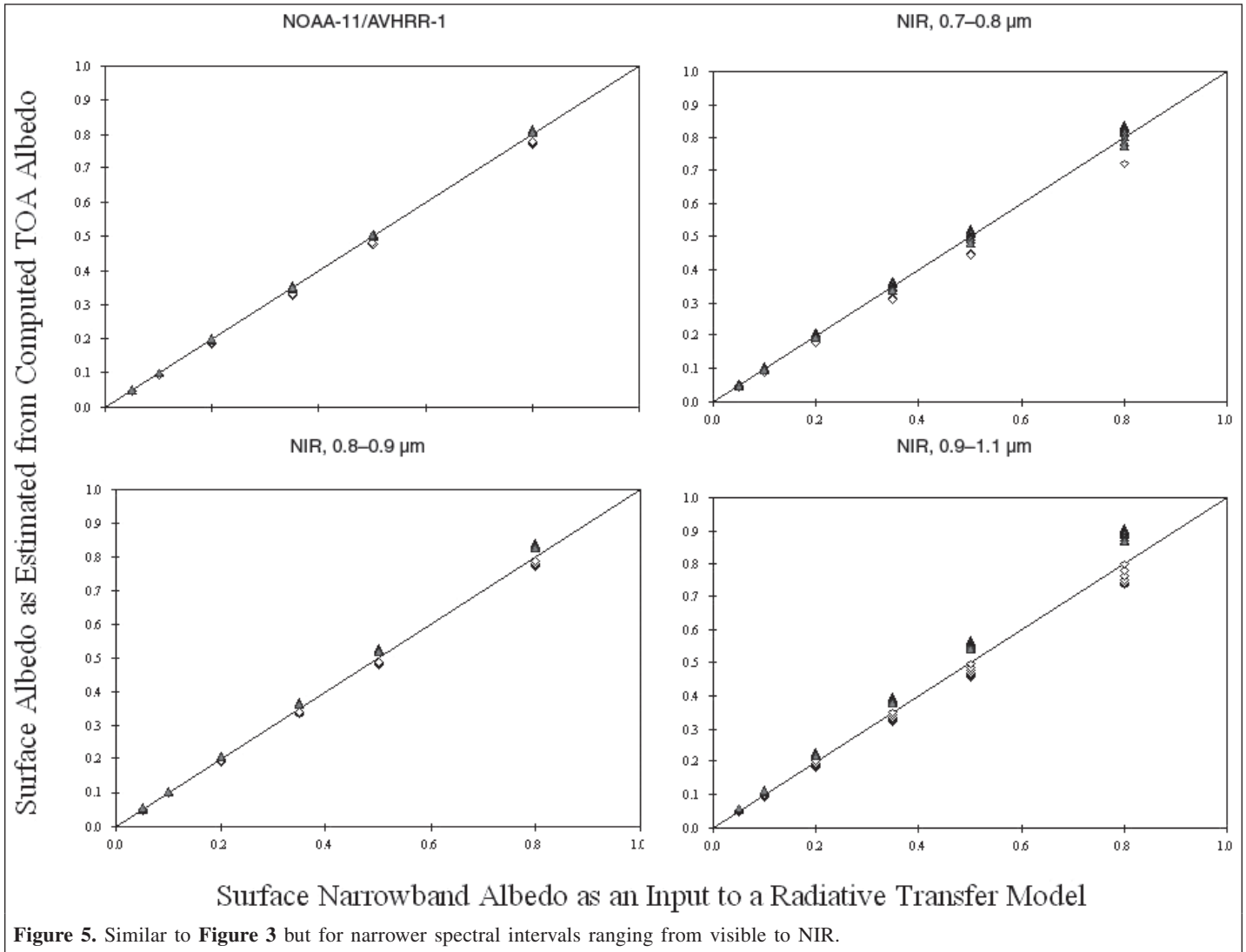
Conclusions

Knowledge of surface spectral albedo (SSA) is required for a variety of climatic, ecological, and environmental studies. To obtain SSA from satellite observations requires an inversion algorithm to account for the effects of the intervening atmosphere. The majority of inversion algorithms were designed for particular sensors or spectral regions using either highly simplified models or detailed complex models. A generalized model of intermediate complexity has been lacking. This paper presents a general inversion model for retrieving SSAs in any spectral region.

From a three-layer atmosphere–surface system, an analytical relationship can be established between albedos at the top and bottom of the atmosphere. Solving the relationship requires determination of reflectance and transmittance in each layer. Major absorption and scattering processes are parameterized such as absorption due to water vapour and ozone and Rayleigh







scattering. Complications arise in determining band-mean transmittance, which was dealt with by separating downward and upward direct and diffuse fluxes in each layer. The parameterized model was evaluated against a detailed radiative transfer model by comparing SSAs as input for the radiative transfer model with those estimated by the approximate inversion algorithm, which used TOA albedo simulated by the detailed model. The inversion model proved to be generally valid over a wide range of spectral intervals from UV to the total solar spectrum, with relatively large errors occurring only for wide bands that contain highly variable absorption.

Acknowledgements

The study was supported by the US Department of Energy Atmospheric Radiation Program with grants DEFG0201ER63166 and DEFG0202ER63351 and National Aeronautics and Space Administration (NASA) grant NNG04GE79G.

References

Barker, H.W., and Davies, J.A. 1989. Surface albedo estimates from Nimbus-7 ERB data and a two-stream approximation of the radiative transfer equation. *Journal of Climate*, Vol. 2, pp. 409–418.

Barker, H.W., Stephens, G.L., Partain, P.T., Bergman, J.W., Bonnel, B., Campana, K., Clothiaux, E.E., Clough, S., Cusack, S., Delamere, J., Edwards, J., Evans, K.F., Fouquart, Y., Freidenreich, S., Galin, V., Hou, Y., Kato, S., Li, J., Mlawer, E., Morcrette, J.-J., O’Hirok, W., Räisänen, P., Ramaswamy, V., Ritter, B., Rozanov, E., Schlesinger, M., Shibata, K., Sporyshev, P., Sun, Z., Wendisch, M., Wood, N., and Yang, F. 2003. Assessing 1D atmospheric solar radiative transfer models: interpretation and handling of unresolved clouds. *Journal of Climate*, Vol. 16, pp. 2676–2699.

Chang, F.-L., Li, Z., and Trishchenko, A. 2000. The dependence of TOA anisotropic reflection on cloud properties inferred from ScaRaB satellite data. *Journal of Applied Meteorology*, Vol. 39, pp. 2480–2493.

Chen, T.S., and Ohring, G. 1984. On the relationship between clear sky planetary and surface albedos. *Journal of Atmospheric Sciences*, Vol. 41, pp. 156–158.

- Cihlar, J., Chen, J., Li, Z., Huang, F., and Pokrant, H. 1997a. Can interannual land surface signal be discerned in composite AVHRR data? *Journal of Geophysical Research*, Vol. 103, pp. 23 163 – 23 172.
- Cihlar, J., Beaubien, J., Xiao, Q., Chen, J., and Li, Z. 1997b. Land cover of the BOREAS region from AVHRR and LANDSAT data. *Canadian Journal of Remote Sensing*, Vol. 23, pp. 163–175.
- Ciren, P., and Li, Z. 2001. The TOA anisotropic reflection of UV radiation, characteristics and models obtained from Meteor-3/TOMS. *Journal of Geophysical Research*, Vol. 106, pp. 4741–4755.
- Dickerson, R.E. 1983. Land surface processes and climate-surface albedos and energy balance. *Advances in Geophysics*, Vol. 25, pp. 305–353.
- Dickerson, R.E., Pinty, B., and Verstraete, M.M. 1990. Relating surface albedos in GCMs to remotely sensed data. *Agricultural and Forest Meteorology*, Vol. 52, pp. 109–131.
- Hansen, J.E., Russell, D., Rind, D., Stone, P., Lacis, A., Travis, L., Lebedeff, S., and Ruedy, R. 1983. Efficient three-dimensional global models for climate studies: models I and II. *Monthly Weather Review*, Vol. 111, pp. 609–662.
- Huete, A., Didan, K., Miura, T., Rodrigue, E.P., Gao, X., and Ferreira, L.G. 2002. Overview of the radiometric and biophysical performance of the MODIS vegetation indices. *Remote Sensing of Environment*, Vol. 83, pp. 195–213.
- Jeong, M.-J., and Li, Z. 2005. Quality, compatibility and synergy analyses of global aerosol products derived from the advanced very high resolution radiometers and total ozone mapping spectrometers. *Journal of Geophysical Research*, Vol. 110, No. D10S08, doi:10.1029/2004JD00464.
- Joseph, J.H., Wiscombe, W.J., and Weinman, J.A. 1976. The delta-Eddington approximation for radiative transfer. *Journal of the Atmospheric Sciences*, Vol. 33, pp. 2452–2459.
- Kaufman, Y.J., Tanré, D., and Boucher, O. 2002. A satellite view of aerosols in the climate system. *Nature (London)*, Vol. 419, pp. 215–223.
- King, M.D., Menzel, W.P., Kaufman, Y.J., Tanré, D., Gao, B.C., Platnick, S., Ackerman, S.A., Remer, L.A., Pincus, R., and Hubanks, P.A. 2003. Cloud and aerosol properties, precipitable water, and profiles of temperature and humidity from MODIS. *IEEE Transactions on Geoscience and Remote Sensing*, Vol. 41, pp. 442–458.
- Leighton, H.G. 1980. Application of the delta-Eddington method to the absorption of solar radiation in the atmosphere. *Atmosphere–Ocean*, Vol. 18, pp. 43–52.
- Li, Z., and Garand, L. 1994. Estimation of surface albedo from space: a parameterization for global application. *Journal of Geophysical Research*, Vol. 99, pp. 8335–8350.
- Li, Z., and Trishchenko, A. 1999. A study towards an improved understanding of the relationship between visible and SW albedo measurements. *Journal of Atmospheric and Oceanic Technology*, Vol. 16, pp. 347–360.
- Li, Z., Moreau, L., Cihlar, J. 1997a. Estimation of the photosynthetically active radiation absorbed at the surface over the BOREAS region. *Journal of Geophysical Research*, Vol. 102, pp. 29 717 – 29 727.
- Li, Z., Moreau, L., and Arking, A. 1997b. On solar energy disposition, a perspective from observation and modeling. *Bulletin of the American Meteorological Society*, Vol. 78, pp. 53–70.
- Li, X., Gao, F., Wang, J., and Strahler, A.H. 2001. A priori knowledge accumulation and its application to linear BRDF model inversions. *Journal of Geophysical Research*, Vol. D106, pp. 11 925 – 11 935.
- Li, Z., Cribb, M., and Trishchenko, A. 2002. Impact of surface inhomogeneity on solar radiative transfer under overcast conditions. *Journal of Geophysical Research*, Vol. 107, No. D16, doi:10.1029/2001JD000976.
- Liang, S. 2003. A direct algorithm for estimating land surface broadband albedos from MODIS imagery. *IEEE Transactions on Geoscience and Remote Sensing*, Vol. 41, pp. 136–145.
- Liang, S., Strahler, A., and Walthall, C. 1999. Retrieval of land surface albedo from satellite observations: a simulation study. *Journal of Applied Meteorology*, Vol. 38, pp. 712–725.
- Liang, S., Yu, Y., and Defelice, T.P. 2005. VIIRS narrowband to broadband land surface albedo conversion: formula and validation. *International Journal of Remote Sensing*, Vol. 26, No. 5, pp. 1019–1025.
- Lucht, W., Schaaf, C.B., and Strahler, A.H. 2000. An algorithm for the retrieval of albedo from space using semiempirical BRDF models. *IEEE Transactions on Geoscience and Remote Sensing*, Vol. 38, pp. 977–998.
- Luo, Y., Trishchenko, A.P., Latifovic, R., and Li, Z. 2005. Surface bidirectional reflectance and albedo properties derived using a land cover-based approach with moderate resolution imaging spectroradiometer observations. *Journal of Geophysical Research*, Vol. 110, No. D01106, doi:10.1029/2004JD004741.
- Meador, M.E., and Weaver, W.R. 1980. Two-stream approximations to radiative transfer in planetary atmospheres: a unified description of existing methods and a new improvement. *Journal of the Atmospheric Sciences*, Vol. 37, pp. 630–643.
- Mishchenko, M.I., Geogdzhayev, I.V., Liu, L., Ogren, J.A., Lacis, A.A., Rossow, W.B., Hovenier, J.W., Volten, H., and Munoz, O. 2003. Aerosol retrievals from AVHRR radiances: effects of particle nonsphericity and absorption and an updated long-term global climatology of aerosol properties. *Journal of Quantitative Spectroscopy and Radiative Transfer*, Vol. 79–80, pp. 953–972.
- Nakajima, T., and Higurashi, A. 1998. A use of two-channel radiances for an aerosol characterization from space. *Geophysical Research Letters*, Vol. 25, No. 20, pp. 3815–3818.
- Pinker, R., and Laszlo, I. 1992. Modeling surface solar irradiance for satellite applications on a global scale. *Journal of Applied Meteorology*, Vol. 31, pp. 194–211.
- Remer, L.A., Kaufman, Y.J., Tanré, D., Mattoo, S., Chu, D.A., Martins, J.V., Li, R.-R., Ichoku, C., Levy, R.C., Kleidman, R.G., Eck, R.F., Vermote, E., and Holben, B.N. 2005. The MODIS aerosol algorithm, products and validation. *Journal of the Atmospheric Sciences*, Vol. 62, pp. 947–973.
- Schaaf, C.B., Gao, F., Strahler, A.H., Lucht, W., Li, X., Tsang, T., Strugnell, N.C., Zhang, X., Jin, Y., Muller, J.-P., Lewis, P., Barnsley, M., Hobson, P., Disney, M., Roberts, G., Dunderdale, M., Doll, C., d'Entremont, R., Hu, B., Liang, S., and Privette, J.L. 2002. First operational BRDF, albedo and nadir reflectance products from MODIS. *Remote Sensing of Environment*, Vol. 83, pp. 135–148.
- Sellers, P.J. 1985. Canopy reflectance, photosynthesis and transpiration. *International Journal of Remote Sensing*, Vol. 6, pp. 1335–1372.
- Trishchenko, A.P., Cihlar, J., and Li, Z. 2002. Effects of spectral response function on surface reflectance and NDVI measured with moderate resolution satellite sensors. *Remote Sensing of Environment*, Vol. 81, pp. 1–18.
- Vermote, E.F., El Saleous, N.Z., Justice, C.O., Kaufman, Y.J., Privette, J., Remer, L., Roger, J.C., and Tanré, D. 1997. Atmospheric correction of visible to middle infrared EOS-MODIS data over land surface, background, operational algorithm and validation. *Journal of Geophysical Research*, Vol. 102, pp. 17 131 – 17 141.